

Article

Design, Synthesis and Antitumor Activity of Quercetin Derivatives Containing a Quinoline Moiety

Wenting Zhang ^{1,2}, Jian Sun ^{1,*}, Peng Zhang ², Ruixue Yue ¹, Yi Zhang ¹, Fuxiang Niu ¹, Hong Zhu ¹, Chen Ma ¹ and Shaoying Deng ¹

¹ Xuzhou Institute of Agricultural Sciences in Jiangsu Xuhuai District, Xuzhou 221131, China; 20171002@jaas.ac.cn (W.Z.)

² School of Life Sciences, Jiangsu Normal University, Xuzhou 221008, China

* Correspondence: xzsunjian@jaas.ac.cn

Abstract: Quercetin is a flavonoid with significant biological and pharmacological activity. In this paper, quercetin was modified at the 3-OH position. Rutin was used as a raw material. We used methyl protection, Williamson etherification reactions, and then substitution reactions to prepare 15 novel quercetin derivatives containing a quinoline moiety. All these complexes were characterized by ¹H NMR, ¹³C NMR, IR and HRMS. Of these, compound **3e** ($IC_{50} = 6.722 \mu\text{mol}\cdot\text{L}^{-1}$) had a better inhibitory effect on human liver cancer (HepG-2) than DDP (Cisplatin) ($IC_{50} = 26.981 \mu\text{mol}\cdot\text{L}^{-1}$). The mechanism of the action experiment showed that compound **3e** could induce cell apoptosis.

Keywords: quercetin; quinoline; antitumor activity; synthesis

1. Introduction

Flavonoids are a widely distributed class of phytochemicals with important medicinal properties such as anti-inflammatory [1], anti-aging [2], and antioxidative [3] properties. Quercetin (3,3',4',5,7-pentahydroxyflavone) is one of the most important flavonoids in the human diet. It belongs to polyphenolic flavonoids that are abundantly found in apples, red grapes, onions, citrus fruits, and green leafy vegetables. It has various biological effects including anti-tumor [4–6], anti-inflammatory [7,8], antiviral [9,10], and antiplatelet aggregation [11] effects.

Research has shown that quercetin can treat and prevent various cancers including prostate cancer alone or in combination with other dietary natural products [12,13]. The potential mechanism of its anti-proliferative effect on prostate cancer cells is related to its impacts on the cell cycle, apoptosis, and regulation of androgen receptors [14]. Studies based on cells and animals, as well as clinical studies, have confirmed the medicinal value of quercetin as an anti-prostate cancer drug. However, *in vivo* and *in vitro* data demonstrated that its moderate potency hindered its further development [15].

Therefore, the chemical structure of quercetin should be modified. The literature shows that the introduction of one substituent group to the phenolic hydroxyl group of quercetin—especially lengthy and/or bulky groups—might be an effective strategy for the modification of quercetin as an anticancer drug [16].

Quercetin has a B ring with an *o*-diphenol structure. The A ring has an *m*-diphenol structure. The phenolic hydroxyl groups of the A and B rings of quercetin play an important role in anti-oxidation [17]. The C ring contains enol and ketone structures, which gives quercetin some special biological activities. The derivatives obtained by modifying different groups have different biological activities and efficacies [18]. 3-OH is the unique hydroxyl group of quercetin, and in this study, chemical modifications are carried out at this position.

Quinoline is a nitrogen-containing heterocyclic aromatic compound with distinct biological activities such as antimarial [19], antibacterial [20], analgesic [21], anti-inflammatory [22],



Citation: Zhang, W.; Sun, J.; Zhang, P.; Yue, R.; Zhang, Y.; Niu, F.; Zhu, H.; Ma, C.; Deng, S. Design, Synthesis and Antitumor Activity of Quercetin Derivatives Containing a Quinoline Moiety. *Molecules* **2024**, *29*, 240. <https://doi.org/10.3390/molecules29010240>

Academic Editor: Robert Musiol

Received: 18 October 2023

Revised: 28 November 2023

Accepted: 30 November 2023

Published: 2 January 2024



Copyright: © 2024 by the authors. Licensee MDPI, Basel, Switzerland. This article is an open access article distributed under the terms and conditions of the Creative Commons Attribution (CC BY) license (<https://creativecommons.org/licenses/by/4.0/>).

antineoplastic [23], and antifungal [24] activities. Some approved drugs contain quinoline skeletons including the fluoroquinolone antibiotics ciprofloxacin (1), norfloxacin (2), levofloxacin (3), gatifloxacin (4), pitavastatin (5), lenvatinib (6), finafloxacin (7), imiquimod (8), indacaterol (9), amsacrine (10), and hydroxychloroquine (11). The structures of compounds (1–11) are presented in Figure 1. Research has shown that quinoline derivatives have excellent antiviral activity against Dengue virus [25], Zika virus [26], Avian influenza virus [27], and COVID-19 [28,29]. Therefore, quinoline and its analogs are worthy of attention in the field of drug discovery and development.

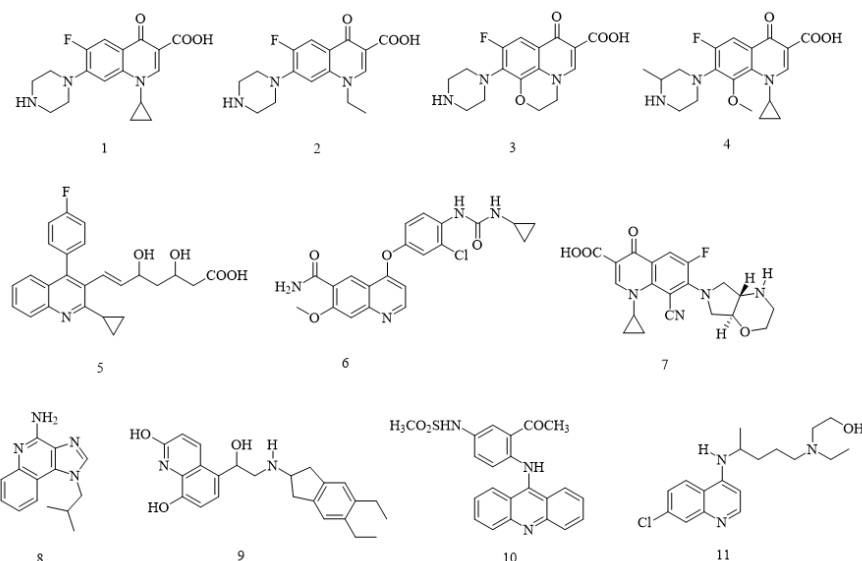


Figure 1. Structure of quinoline (1–11)-based approved drugs.

We thus speculated that introducing hydroxyquinoline fragments into quercetin might generate novel lead compounds with greater biological activities. Thus, 15 derivatives of quercetin containing quinoline groups were synthesized by introducing quinoline active groups into the 3-OH group of quercetin through an active splicing method. The anti-tumor activities of the target compounds were tested to find compounds with good anti-tumor activities, which provide a theoretical basis for related work.

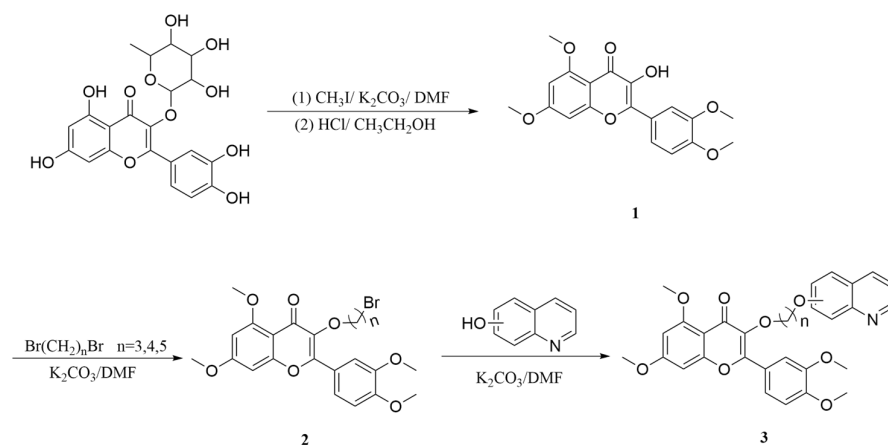
2. Results and Discussion

2.1. Chemistry

The synthetic routes are shown in Scheme 1. Rutin underwent methylation and deglycosylation steps to obtain intermediate 1. Midbody 2 was obtained by reacting 1,3-dibromopropane or 1,4-dibromobutane or 1,5-dibromopentane with 1. The target compound 3 was obtained by the substitution reaction of 2 with hydroxyquinoline under alkaline conditions.

The structures of **3a–3o** were characterized by ^1H nuclear magnetic resonance (NMR), ^{13}C NMR, and high-resolution mass spectrometry (HRMS); detailed data are included in the Supplementary Materials. For example, the ^1H NMR spectra of compound **3a**, taken as a typical example of the series, showed 33 signals at δ 1.53–1.45 (m, 2H, CH_2), 1.62 (td, J = 7.7, 14.9 Hz, 2H, CH_2), 1.71 (quin, J = 6.9 Hz, 2H, CH_2), 3.84 (s, 3H, CH_3), 3.89 (s, 9H, 3 CH_3), 3.93 (t, J = 6.4 Hz, 2H, CH_2), 4.23–4.16 (m, 2H, CH_2), 6.49 (d, J = 2.3 Hz, 1H, Ar-H), 6.59 (d, J = 9.5 Hz, 1H, chromene-H), 6.82 (d, J = 2.3 Hz, 1H, Ar-H), 7.14 (d, J = 8.6 Hz, 1H, Ar-H), 7.28–7.22 (m, 1H, quinoline-H), 7.55–7.51 (m, 1H, quinoline-H), 7.63–7.58 (m, 1H, quinoline-H), 7.73–7.65 (m, 3H, quinoline-H), and 7.89 (d, J = 9.5 Hz, 1H, chromene-H). Meanwhile, the ^{13}C NMR spectra of **3a** showed the corresponding carbonyl carbons around δ 172.7 ppm, aromatic carbon around δ 164.1, 161.4, 160.8, 158.6, 152.3, 151.1, 148.8, 140.0, 139.8, 139.3, 131.3, 129.5, 123.1, 122.3, 122.0, 121.5, 120.8, 115.0, 111.9, 116.0, 108.9 ppm,

alkene carbon around δ 96.4, 93.5 ppm, methoxy carbon around δ 71.8, 56.6, 56.5, 56.1 ppm, and methylene carbon around δ 41.7, 30.9, 29.8, 28.6, 22.7 ppm.



Scheme 1. Synthetic route of target compounds **3**.

2.2. Anti-Tumor Activity In Vitro

The anti-tumor activity of all the target compounds **3a–3o** was evaluated in vitro by an MTT assay against HepG-2, A549, and MCF-7 cell lines, with DDP as the positive control. Their inhibition rate and IC₅₀ values are listed in Table 1.

Table 1. Inhibition rate of target compound on proliferation of different tumor cells.

No.	Compd.	n	OH	IC ₅₀ /($\mu\text{mol}\cdot\text{L}^{-1}$) ^a				
				HepG-2	THLE-2	A549	HBE	MCF-7
1	3a	5	2-OH	10.600	35.552	7.384	8.120	1.607
2	3b	5	3-OH	26.003	115.084	>100	>100	6.793
3	3c	5	4-OH	>100	>100	>100	>100	>100
4	3d	5	6-OH	36.621	83.421	>100	>100	>100
5	3e	5	7-OH	6.722	92.836	26.614	0.873	3.004
6	3f	3	2-OH	>100	>100	>100	>100	>100
7	3g	3	3-OH	>100	>100	>100	>100	>100
8	3h	3	4-OH	>100	>100	31.678	8.432	>100
9	3i	3	6-OH	5.074	>100	>100	>100	6.464
10	3j	3	7-OH	>100	23.442	>100	>100	48.001
11	3k	4	2-OH	5.193	46.792	>100	>100	6.856
12	3l	4	3-OH	>100	>100	>100	>100	>100
13	3m	4	4-OH	>100	>100	>100	>100	>100
14	3n	4	6-OH	>100	>100	>100	>100	>100
15	3o	4	7-OH	>100	>100	>100	>100	>100
16	Quercetin			>100	>100	>100	>100	>100
17	DDP ^b			26.981		48.523		2.940

^a IC₅₀ ($\mu\text{mol}\cdot\text{L}^{-1}$): the concentration of compound required for cell activity to be suppressed by half;
^b DDP: positive control.

The inhibitory effect of partially synthesized quercetin derivatives containing quinoline structures on HepG-2 cells, A549, and MCF-7 cell lines was higher than that of quercetin and DDP. The inhibitory effects of **3i**, **3k**, and **3e** on HepG-2 cells were stronger than

those of DDP and quercetin, with IC₅₀ values of 5.074 $\mu\text{mol}\cdot\text{L}^{-1}$, 5.193 $\mu\text{mol}\cdot\text{L}^{-1}$, and 6.722 $\mu\text{mol}\cdot\text{L}^{-1}$, respectively. The inhibitory effects of **3a**, **3e**, and **3h** on A549 cells were stronger than those of DDP and quercetin, with IC₅₀ values of 7.384 $\mu\text{mol}\cdot\text{L}^{-1}$, 26.614 $\mu\text{mol}\cdot\text{L}^{-1}$, and 31.678 $\mu\text{mol}\cdot\text{L}^{-1}$, respectively. **3a** had a stronger inhibitory effect on MCF-7 cells than DDP, with an IC₅₀ value of 1.607 $\mu\text{mol}\cdot\text{L}^{-1}$. The inhibitory effect of **3e**, **3i**, **3b**, and **3k** on MCF-7 cells was stronger than that of quercetin, with IC₅₀ values of 3.004 $\mu\text{mol}\cdot\text{L}^{-1}$, 6.464 $\mu\text{mol}\cdot\text{L}^{-1}$, 6.793 $\mu\text{mol}\cdot\text{L}^{-1}$, and 6.856 $\mu\text{mol}\cdot\text{L}^{-1}$, respectively. Specifically, compound **3e** had a higher inhibitory rate on HepG-2 and less toxicity to normal cells; thus, **3e** was chosen as the lead compound for the next step of research.

2.3. Compound **3e** Induces HepG-2 Cell Apoptosis

Most anticancer drugs can kill tumor cells by inducing cell apoptosis, and thus, inducing cell apoptosis is considered one of the main mechanisms for killing tumor cells. Compound **3e** was tested to clarify whether the inhibitory effects of these compounds on cell proliferation were related to apoptosis. HepG-2 cells were treated with DMSO or different concentrations of **3e** for 48 h. Cells were stained with Annexin-V and PI, and the proportion of apoptotic cells was detected by flow cytometry.

Figure 2A,B shows that the HepG-2 cell apoptosis gradually increased (32.2%, 48.4%, and 56.3%) when the concentration of compound **3e** increased (4, 7 and 10 $\mu\text{mol}\cdot\text{L}^{-1}$, respectively). These results indicated that compound **3e** could induce HepG-2 cell apoptosis in a concentration-dependent manner.

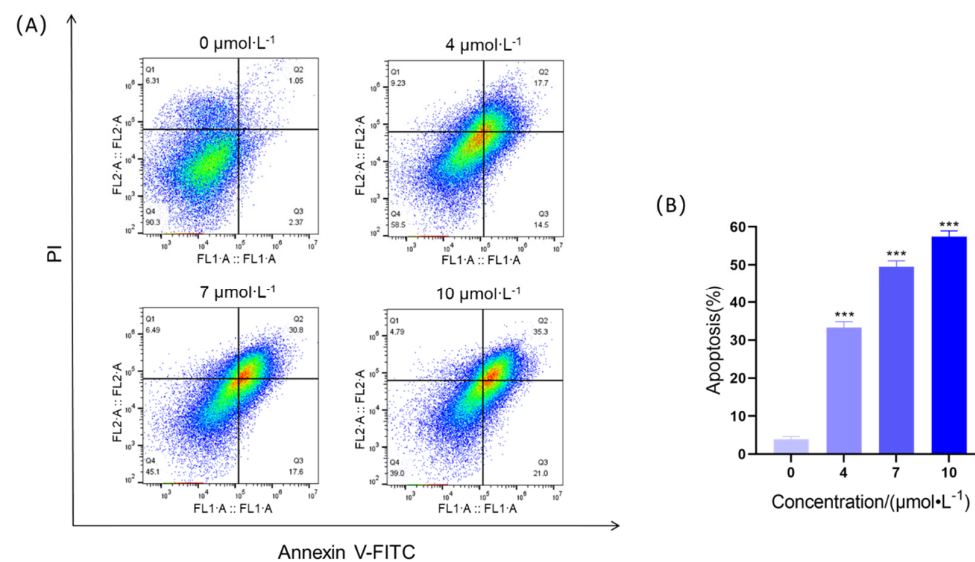


Figure 2. (A) The effect on cellular apoptosis after HepG-2 cells were incubated with compound **3e** for 48 h; (B) statistic histogram indicated the percentages of apoptotic cells (compared with the control group, *** $p < 0.001$).

2.4. Structure–Activity Relationship (SAR) Analysis

As indicated in Table 1, the anti-tumor activities of target compounds were greatly affected by structural variations. Comparing IC₅₀ for compounds **3a**–**3o**, overall, increasing the length of the product alkane bridge was beneficial for enhancing activity. For instance, under the same conditions of R = 2-OH, the target compounds **3a** (R = 2-OH, n = 5) had higher anti-tumor activity against MCF-7 than **3k** (R = 2-OH, n = 4) and **3f** (R = 2-OH, n = 3), with inhibition rates of 1.607 $\mu\text{mol}\cdot\text{L}^{-1}$, 6.856 $\mu\text{mol}\cdot\text{L}^{-1}$ and $>100 \mu\text{mol}\cdot\text{L}^{-1}$, respectively. In addition, for some target compounds, when the OH was substituted at the 2- position of quinoline, the compounds exhibited greater anti-tumor activity. For example, the target compounds **3k** (R = 2-OH, n = 4) had higher anti-tumor activity against HepG-2 (IC₅₀ = 5.193 $\mu\text{mol}\cdot\text{L}^{-1}$) and MCF-7 (IC₅₀ = 6.856 $\mu\text{mol}\cdot\text{L}^{-1}$) than

the products of OH substituted at other positions. However, on the contrary, there were also different situations. For example, the IC₅₀ value of target compound **3i** ($R = 6\text{-OH}$, $n = 3$) on HepG-2 was $5.074 \mu\text{mol}\cdot\text{L}^{-1}$, which was superior to other substituent groups.

2.5. Discussion

Although quercetin demonstrates varied biological activities and pharmacological values, due to its molecular structure, it has poor water solubility and low bioavailability after entering the body, which affects the original efficacy of the drug and limits its application in the pharmaceutical field. Therefore, using quercetin as the lead compound to chemically modify its structure and search for high bioavailability and stronger activity precursor drugs has become a research hotspot in fields of medicine. 3-OH is a unique hydroxyl group of quercetin, and introducing functional groups at this position often yields more active compounds. For instance, Rajaram et al. [15] and Al Jabban et al. [30] alkylated the 3-OH group of quercetin to obtain novel quercetin derivatives with higher anticancer activity.

The research suggested that 3-OH substitution of quercetin could significantly alter its anticancer activities. However, these reports introduced smaller volume groups into the 3-OH group of quercetin. Reports indicated that introducing larger active groups, such as quinazolinone and heterocycle, into the flavonol compounds would effectively enhance their antibacterial, anticancer, and other activities [31,32]. In our study, we selected larger volume quinoline groups and bridged them with alkyl chains of different chain lengths to introduce them into the quercetin molecule. The results indicated that augmenting the length of the alkane bridge was beneficial for improving activity, consistent with the conclusion of Jiang et al. [33].

3. Experimental Section

3.1. Chemistry

Melting points (M.p.) were determined on a Buchi-Tottoli apparatus and were uncorrected. IR spectra were recorded on a Tensor 27 (Bruker Optics, Ettlingen, Germany) spectrometer in KBr pellets. ¹H NMR spectra were obtained from a solution in DMSO-*d*₆ with Me₄Si as the internal standard using a Bruker-400 spectrometer. HRMS analyses used a TOF-Q-MS analyzer (micro-TOF-QII, Bruker, Billerica, MA, US), and the values are expressed as [M + H]⁺. All starting materials were purchased from Saen Chemical Technology (Shanghai, China) Co., Ltd. The reaction courses and product mixtures were routinely monitored by TLC on silica gel (precoated F254 Merck plates). Organic solutions were dried over anhydrous Na₂SO₄.

3.2. General Synthesis Procedure for Intermediates **1** and **2**

Rutin with a purity of 98% was used as a raw material. Intermediates **1** and **2** were synthesized by methods reported in the literature [32,34,35].

3.3. General Synthesis Procedure for Target Product **3**

Intermediate **2** (1.0 mmol), hydroxyquinoline (1.2 mmol, 1.2 eq), and K₂CO₃ (3.0 mmol, 3.0 eq) were added to 20 mL of DMF and reacted at 60 °C for 10–15 h. The reaction was controlled by the TLC method. After the reaction was completed, the mixture was poured into 250 mL of ice water, producing a slight yellow solid. The crude product was obtained through vacuum suction filtration and drying. Finally, target product **3** was purified by column chromatography (CC) (ethyl acetate (EA): methanol (ET) = 11: 1~8: 1, *v/v*).

2-(3,4-dimethoxyphenyl)-5,7-dimethoxy-3-((5-(quinolin-2-yloxy)pentyl)oxy)-4*H*-chromen-4-one (3a**):** CC (EA/ET = 10: 1). Yield 78%, M.p. 209–211 °C; ¹H NMR (DMSO-*d*₆, 400 MHz): δ_H = 7.89 (d, *J* = 9.5 Hz, 1H), 7.73–7.65 (m, 3H), 7.63–7.58 (m, 1H), 7.55–7.51 (m, 1H), 7.28–7.22 (m, 1H), 7.14 (d, *J* = 8.6 Hz, 1H), 6.82 (d, *J* = 2.3 Hz, 1H), 6.59 (d, *J* = 9.5 Hz, 1H), 6.49 (d, *J* = 2.3 Hz, 1H), 4.23–4.16 (m, 2H), 3.93 (t, *J* = 6.4 Hz, 2H), 3.89 (s, 3H), 3.84 (s, 9H), 1.71 (quin, *J* = 6.9 Hz, 2H), 1.62 (td, *J* = 7.7, 14.9 Hz, 2H), 1.53–1.45 (m, 2H). ¹³C NMR (DMSO-*d*₆, 100 MHz): δ_C 172.7, 164.1, 161.4, 160.8,

158.6, 152.3, 151.1, 148.8, 140.0, 139.8, 139.3, 131.3, 129.5, 123.1, 122.3, 122.0, 121.5, 120.8, 115.0, 111.9, 116.0, 108.9, 96.4, 93.5, 71.8, 56.6, 56.5, 56.1, 41.7, 30.9, 29.8, 28.6, 22.7. IR (KBr): ν 3055, 3000, 2939, 2865, 1625, 1602, 1515, 1492, 1451, 1428, 1380, 1353, 1306, 1266, 1254, 1213, 1177, 1142, 1106, 1023, 976, 842, 800, 769, 706 cm⁻¹. HRMS (ESI, *m/z*): Calcd for C₃₃H₃₄NO₈ [M + H]⁺ 572.2284, found 572.2284.

2-(3,4-dimethoxyphenyl)-5,7-dimethoxy-3-((5-(quinolin-3-yloxy)pentyl)oxy)-4H-chromen-4-one (3b): CC (EA/ET = 11: 1). Yield 81%, M.p. 232~234 °C; ¹H NMR (DMSO-*d*₆, 400 MHz): δ _H 8.61 (d, *J* = 2.9 Hz, 1H), 7.97–7.91 (m, 1H), 7.90–7.84 (m, 1H), 7.74 (d, *J* = 2.8 Hz, 1H), 7.70–7.66 (m, 2H), 7.58–7.54 (m, 2H), 7.11 (d, *J* = 8.4 Hz, 1H), 6.81 (d, *J* = 2.3 Hz, 1H), 6.48 (d, *J* = 2.3 Hz, 1H), 4.10 (t, *J* = 6.4 Hz, 2H), 3.96 (t, *J* = 6.3 Hz, 2H), 3.89 (s, 3H), 3.83 (d, *J* = 4.1 Hz, 6H), 3.79 (s, 3H), 1.84–1.72 (m, 4H), 1.60–1.53 (m, 2H). ¹³C NMR (DMSO-*d*₆, 100 MHz): δ _C 172.7, 164.1, 160.8, 158.7, 152.7, 152.4, 151.1, 148.8, 144.7, 143.3, 139.3, 129.2, 129.1, 127.49, 127.47, 127.0, 123.2, 122.0, 113.7, 111.87, 111.83, 109.0, 96.4, 93.5, 71.8, 68.4, 56.6, 56.1, 56.0, 30.9, 29.8, 28.6, 22.7. IR (KBr): ν 3054, 3000, 2942, 2874, 2836, 1624, 1516, 1493, 1466, 1380, 1352, 1265, 1213, 1177, 1161, 1059, 975, 944, 864, 849, 822, 784, 771, 665, 614 cm⁻¹. HRMS (ESI, *m/z*): Calcd for C₃₃H₃₄NO₈ [M + H]⁺ 572.2284, found 572.2280.

2-(3,4-dimethoxyphenyl)-5,7-dimethoxy-3-((5-(quinolin-4-yloxy)pentyl)oxy)-4H-chromen-4-one (3c): CC (EA/ET = 10: 1). Yield 77%, M.p. 200~202 °C; ¹H NMR (DMSO-*d*₆, 400 MHz): δ _H 8.71 (d, *J* = 5.1 Hz, 1H), 8.13 (dd, *J* = 0.9, 8.4 Hz, 1H), 7.93 (d, *J* = 8.4 Hz, 1H), 7.77–7.64 (m, 3H), 7.58–7.50 (m, 1H), 7.07 (d, *J* = 8.5 Hz, 1H), 6.99 (d, *J* = 5.3 Hz, 1H), 6.80 (d, *J* = 2.3 Hz, 1H), 6.48 (d, *J* = 2.3 Hz, 1H), 4.21 (t, *J* = 6.3 Hz, 2H), 3.97 (t, *J* = 6.4 Hz, 2H), 3.89 (s, 3H), 3.84 (s, 3H), 3.81 (s, 3H), 3.77 (s, 3H), 1.93–1.84 (m, 2H), 1.81–1.73 (m, 2H), 1.65–1.58 (m, 2H). ¹³C NMR (DMSO-*d*₆, 100 MHz): δ _C 172.7, 164.1, 161.2, 160.8, 158.7, 152.4, 152.1, 151.1, 149.2, 148.8, 139.9, 130.1, 129.1, 126.1, 125.4, 123.2, 122.0, 121.3, 111.82, 111.80, 109.0, 102.0, 96.4, 93.5, 71.8, 68.8, 56.5, 56.1, 56.0, 30.9, 29.8, 28.5, 22.8. IR (KBr): ν 2995, 2948, 1598, 1518, 1490, 1464, 1432, 1382, 1354, 1311, 1289, 1269, 1212, 1180, 1164, 1141, 1074, 977, 935, 908, 829, 752, 668, 614 cm⁻¹. HRMS (ESI, *m/z*): Calcd for C₃₃H₃₄NO₈ [M + H]⁺ 572.2284, found 572.2278.

2-(3,4-dimethoxyphenyl)-5,7-dimethoxy-3-((5-(quinolin-6-yloxy)pentyl)oxy)-4H-chromen-4-one (3d): CC (EA/ET = 9: 1). Yield 72%, M.p. 198~199 °C; ¹H NMR (DMSO-*d*₆, 400 MHz): δ _H 8.72 (dd, *J* = 1.6, 4.3 Hz, 1H), 8.26–8.20 (m, 1H), 7.90 (d, *J* = 9.0 Hz, 1H), 7.72–7.65 (m, 2H), 7.46 (dd, *J* = 4.2, 8.3 Hz, 1H), 7.40–7.32 (m, 2H), 7.11 (d, *J* = 8.4 Hz, 1H), 6.81 (d, *J* = 2.1 Hz, 1H), 6.48 (d, *J* = 2.1 Hz, 1H), 4.07 (t, *J* = 6.4 Hz, 2H), 3.96 (t, *J* = 6.3 Hz, 2H), 3.89 (s, 3H), 3.83 (d, *J* = 4.5 Hz, 6H), 3.79 (s, 3H), 1.83–1.70 (m, 4H), 1.60–1.51 (m, 2H). ¹³C NMR (DMSO-*d*₆, 100 MHz): δ _C 172.7, 164.1, 160.8, 158.7, 157.0, 152.4, 151.1, 148.7, 148.3, 144.2, 139.9, 135.2, 130.8, 129.6, 123.1, 122.7, 122.1, 122.0, 111.8, 111.7, 108.9, 106.7, 96.4, 93.5, 71.8, 68.3, 56.6, 56.5, 56.0, 30.9, 29.8, 28.7, 22.7. IR (KBr): ν 3065, 3001, 2869, 2837, 1622, 1513, 1462, 1420, 1342, 1318, 1288, 1230, 1204, 1193, 1157, 1002, 975, 868, 824, 811, 795, 702, 646 cm⁻¹. HRMS (ESI, *m/z*): Calcd for C₃₃H₃₄NO₈ [M + H]⁺ 572.2284, found 572.2277.

2-(3,4-dimethoxyphenyl)-5,7-dimethoxy-3-((5-(quinolin-7-yloxy)pentyl)oxy)-4H-chromen-4-one (3e): CC (EA/ET = 8: 1). Yield 74%, M.p. 199~201 °C; ¹H NMR (DMSO-*d*₆, 400 MHz): δ _H 8.80 (dd, *J* = 1.8, 4.3 Hz, 1H), 8.26 (dd, *J* = 1.3, 8.2 Hz, 1H), 7.86 (d, *J* = 9.0 Hz, 1H), 7.73–7.63 (m, 2H), 7.39–7.32 (m, 2H), 7.22 (dd, *J* = 2.5, 8.9 Hz, 1H), 7.11 (d, *J* = 8.4 Hz, 1H), 6.81 (d, *J* = 2.3 Hz, 1H), 6.48 (d, *J* = 2.1 Hz, 1H), 4.09 (t, *J* = 6.4 Hz, 2H), 3.96 (t, *J* = 6.3 Hz, 2H), 3.89 (s, 3H), 3.83 (d, *J* = 4.1 Hz, 6H), 3.80 (s, 3H), 1.83–1.70 (m, 4H), 1.60–1.52 (m, 2H). ¹³C NMR (DMSO-*d*₆, 100 MHz): δ _C 172.7, 164.1, 160.7, 160.0, 158.6, 152.3, 151.1, 149.9, 148.7, 139.9, 136.1, 129.6, 125.4, 123.5, 123.1, 121.9, 119.9, 119.6, 111.8, 111.7, 108.9, 108.2, 96.3, 93.4, 71.7, 68.2, 56.5, 56.0, 34.9, 30.9, 29.8, 28.7, 22.8. IR (KBr): ν 3067, 3002, 2943, 2854, 1624, 1510, 1452, 1396, 1343, 1321, 1303, 1269, 1211, 1105, 1058, 1020, 977, 926, 876, 821, 800, 769, 736, 665, 617 cm⁻¹. HRMS (ESI, *m/z*): Calcd for C₃₃H₃₄NO₈ [M + H]⁺ 572.2284, found 572.2285.

2-(3,4-dimethoxyphenyl)-5,7-dimethoxy-3-(3-(quinolin-2-yloxy)propoxy)-4H-chromen-4-one (3f): CC (EA/ET = 10: 1). Yield 82%, M.p. 223~225 °C; ¹H NMR (DMSO-*d*₆, 400 MHz): δ _H 7.91 (d, *J* = 9.5 Hz, 1H), 7.75–7.67 (m, 3H), 7.63–7.56 (m, 1H), 7.55–7.49 (m, 1H), 7.26 (t, *J* = 7.4 Hz, 1H), 7.15–7.09 (m, 1H), 6.86–6.81 (m, 1H), 6.60 (d, *J* = 9.5 Hz, 1H), 6.53–6.46 (m, 1H), 4.40–4.32 (m, 2H), 4.06 (t, *J* = 6.3 Hz, 2H), 3.90 (s, 3H), 3.86–3.79 (m, 9H), 2.05–1.96 (m, 2H). ¹³C NMR (DMSO-*d*₆, 100 MHz): δ _C 172.6, 164.2, 161.4, 160.8, 158.7, 152.5, 151.2, 148.9, 140.0, 139.8, 139.3, 131.4, 129.6, 123.1, 122.4, 122.0, 121.5, 120.9, 114.7, 112.0, 111.7, 108.9, 96.4, 93.6, 70.0,

64.7, 56.6, 56.5, 56.09, 56.07, 28.5. IR (KBr): ν 2934, 2839, 1651, 1512, 1494, 1453, 1420, 1320, 1271, 1252, 1232, 1211, 1157, 1057, 1002, 980, 887, 827, 770, 745, 648 cm^{-1} . HRMS (ESI, m/z): Calcd for $\text{C}_{31}\text{H}_{30}\text{NO}_8$ [M + H]⁺ 544.1971, found 544.1959.

2-(3,4-dimethoxyphenyl)-5,7-dimethoxy-3-(quinolin-3-yloxy)propoxy-4H-chromen-4-one (3g): CC (EA/ET = 10: 1). Yield 77%, M.p. 209~211 °C; ¹H NMR (DMSO-*d*₆, 400 MHz): δ_{H} 8.58 (d, *J* = 2.9 Hz, 1H), 7.97~7.92 (m, 1H), 7.90~7.84 (m, 1H), 7.65~7.55 (m, 5H), 6.85 (d, *J* = 8.6 Hz, 1H), 6.80 (d, *J* = 2.3 Hz, 1H), 6.48 (d, *J* = 2.3 Hz, 1H), 4.21 (t, *J* = 6.2 Hz, 2H), 4.15 (t, *J* = 6.0 Hz, 2H), 3.89 (s, 3H), 3.84 (s, 3H), 3.79 (s, 3H), 3.62 (s, 3H), 2.21~2.15 (m, 2H). ¹³C NMR (DMSO-*d*₆, 100 MHz): δ_{C} 172.7, 164.2, 160.8, 158.7, 152.6, 152.5, 151.1, 148.8, 144.7, 143.4, 139.8, 129.10, 129.07, 127.52, 127.50, 127.1, 123.0, 122.1, 113.6, 111.73, 111.67, 109.0, 96.4, 93.5, 68.7, 65.3, 56.6, 56.5, 56.1, 55.8, 29.8. IR (KBr): ν 3063, 2882, 2839, 1605, 1514, 1494, 1463, 1425, 1350, 1312, 1272, 1251, 1211, 1162, 1112, 1057, 1003, 936, 848, 819, 785, 705, 616 cm^{-1} . HRMS (ESI, m/z): Calcd for $\text{C}_{31}\text{H}_{30}\text{NO}_8$ [M + H]⁺ 544.1971, found 544.1957.

2-(3,4-dimethoxyphenyl)-5,7-dimethoxy-3-(quinolin-4-yloxy)propoxy-4H-chromen-4-one (3h): CC (EA/ET = 11: 1). Yield 78%, M.p. 229~230 °C; ¹H NMR (DMSO-*d*₆, 400 MHz): δ_{H} 8.69 (d, *J* = 5.3 Hz, 1H), 8.05 (dd, *J* = 1.0, 8.4 Hz, 1H), 7.93 (d, *J* = 8.4 Hz, 1H), 7.72 (ddd, *J* = 1.4, 6.9, 8.4 Hz, 1H), 7.62~7.54 (m, 2H), 7.50 (ddd, *J* = 1.2, 6.9, 8.3 Hz, 1H), 6.89 (d, *J* = 5.3 Hz, 1H), 6.81~6.76 (m, 2H), 6.48 (d, *J* = 2.4 Hz, 1H), 4.32 (t, *J* = 6.1 Hz, 2H), 4.20 (t, *J* = 6.0 Hz, 2H), 3.89 (s, 3H), 3.84 (s, 3H), 3.76 (s, 3H), 3.69 (s, 3H), 2.25 (quin, *J* = 6.1 Hz, 2H). ¹³C NMR (DMSO-*d*₆, 100 MHz): δ_{C} 172.6, 164.2, 161.0, 160.8, 158.7, 152.6, 152.0, 151.1, 149.2, 148.8, 139.8, 130.1, 129.1, 126.1, 123.0, 122.01, 122.00, 121.2, 111.64, 111.60, 109.0, 101.9, 96.4, 93.5, 68.6, 65.5, 56.6, 56.5, 56.1, 55.9, 29.6. IR (KBr): ν 2999, 2960, 1605, 1517, 1483, 1353, 1270, 1212, 1180, 1143, 1117, 1024, 1009, 979, 969, 953, 866, 820, 782, 770, 741, 682 cm^{-1} . HRMS (ESI, m/z): Calcd for $\text{C}_{31}\text{H}_{30}\text{NO}_8$ [M + H]⁺ 544.1971, found 544.1958.

2-(3,4-dimethoxyphenyl)-5,7-dimethoxy-3-(quinolin-6-yloxy)propoxy-4H-chromen-4-one (3i): CC (EA/ET = 10: 1). Yield 80%, M.p. 208~210 °C; ¹H NMR (DMSO-*d*₆, 400 MHz): δ_{H} 8.73 (dd, *J* = 1.6, 4.2 Hz, 1H), 8.22 (d, *J* = 7.4 Hz, 1H), 7.90 (d, *J* = 9.1 Hz, 1H), 7.66~7.59 (m, 2H), 7.47 (dd, *J* = 4.2, 8.3 Hz, 1H), 7.34 (dd, *J* = 2.8, 9.1 Hz, 1H), 7.25 (d, *J* = 2.6 Hz, 1H), 6.87~6.79 (m, 2H), 6.49 (d, *J* = 2.3 Hz, 1H), 4.22~4.11 (m, 4H), 3.89 (s, 3H), 3.84 (s, 3H), 3.79 (s, 3H), 3.62 (s, 3H), 2.20~2.13 (m, 2H). ¹³C NMR (DMSO-*d*₆, 100 MHz): δ_{C} 172.6, 164.1, 160.7, 158.6, 156.8, 152.5, 151.0, 148.8, 148.4, 144.2, 139.7, 135.2, 130.8, 129.5, 123.0, 122.6, 122.1, 122.0, 111.59, 111.55, 108.9, 106.7, 96.4, 93.5, 68.6, 65.1, 56.6, 56.5, 56.0, 55.7, 29.8. IR (KBr): ν 3003, 2938, 2913, 2876, 1632, 1578, 1516, 1490, 1466, 1430, 1379, 1361, 1269, 1179, 1110, 1061, 1040, 1010, 987, 846, 816, 796, 642, 617 cm^{-1} . HRMS (ESI, m/z): Calcd for $\text{C}_{31}\text{H}_{30}\text{NO}_8$ [M + H]⁺ 544.1971, found 544.1955.

2-(3,4-dimethoxyphenyl)-5,7-dimethoxy-3-(quinolin-7-yloxy)propoxy-4H-chromen-4-one (3j): CC (EA/ET = 11: 1). Yield 74%, M.p. 208~210 °C; ¹H NMR (DMSO-*d*₆, 400 MHz): δ_{H} 8.81 (dd, *J* = 1.8, 4.3 Hz, 1H), 8.26 (dd, *J* = 1.3, 8.1 Hz, 1H), 7.86 (d, *J* = 8.9 Hz, 1H), 7.69~7.59 (m, 2H), 7.37 (dd, *J* = 4.3, 8.1 Hz, 1H), 7.31 (d, *J* = 2.3 Hz, 1H), 7.20 (dd, *J* = 2.5, 8.9 Hz, 1H), 6.88 (d, *J* = 8.6 Hz, 1H), 6.80 (d, *J* = 2.1 Hz, 1H), 6.48 (d, *J* = 2.3 Hz, 1H), 4.25~4.20 (m, 2H), 4.15 (t, *J* = 6.1 Hz, 2H), 3.89 (s, 3H), 3.84 (s, 3H), 3.80 (s, 3H), 3.66 (s, 3H), 2.20~2.15 (m, 2H). ¹³C NMR (DMSO-*d*₆, 100 MHz): δ_{C} 172.6, 164.1, 160.7, 159.8, 158.6, 152.5, 151.1, 151.0, 149.9, 148.8, 139.8, 136.1, 129.7, 123.5, 122.9, 122.0, 119.9, 119.7, 111.6, 111.5, 108.9, 108.2, 96.4, 93.5, 68.6, 65.1, 56.6, 56.5, 56.0, 55.7, 29.8. IR (KBr): ν 2954, 1725, 1625, 1514, 1355, 1322, 1306, 1209, 1109, 1046, 1021, 981, 942, 852, 836, 812, 769, 729, 707, 652, 618 cm^{-1} . HRMS (ESI, m/z): Calcd for $\text{C}_{31}\text{H}_{30}\text{NO}_8$ [M + H]⁺ 544.1971, found 544.1956.

2-(3,4-dimethoxyphenyl)-5,7-dimethoxy-3-(4-(quinolin-2-yloxy)butoxy-4H-chromen-4-one (3k): CC (EA/ET = 10: 1). Yield 77%, M.p. 211~212 °C; ¹H NMR (DMSO-*d*₆, 400 MHz): δ_{H} 7.90 (d, *J* = 9.5 Hz, 1H), 7.75~7.70 (m, 1H), 7.69~7.55 (m, 4H), 7.29~7.22 (m, 1H), 7.06 (d, *J* = 8.6 Hz, 1H), 6.81 (d, *J* = 2.1 Hz, 1H), 6.59 (d, *J* = 9.4 Hz, 1H), 6.48 (d, *J* = 2.3 Hz, 1H), 4.28 (br t, *J* = 6.4 Hz, 2H), 3.95 (br t, *J* = 5.3 Hz, 2H), 3.89 (s, 3H), 3.83 (s, 3H), 3.81 (s, 3H), 3.77 (s, 3H), 1.78~1.73 (m, 4H). ¹³C NMR (DMSO-*d*₆, 100 MHz): δ_{C} 172.7, 164.1, 161.4, 160.7, 158.6, 152.4, 151.1, 148.7, 139.9, 139.8, 139.3, 131.3, 129.5, 123.0, 122.3, 121.9, 121.5, 120.8, 115.1, 111.8, 111.5, 108.9, 96.4, 93.5, 71.5, 56.6, 56.5, 56.02, 56.00, 41.5, 27.5, 24.5. IR (KBr): ν 2998, 2937,

2853, 1629, 1511, 1491, 1426, 1380, 1322, 1303, 1268, 1250, 1181, 1107, 1021, 981, 837, 796, 759, 666, 650 cm^{-1} . HRMS (ESI, m/z): Calcd for $\text{C}_{32}\text{H}_{32}\text{NO}_8$ [M + H]⁺ 558.2128, found 558.2112.

2-(3,4-dimethoxyphenyl)-5,7-dimethoxy-3-(4-(quinolin-3-yloxy)butoxy)-4H-chromen-4-one (3l): CC (EA/ET = 10: 1). Yield 73%, M.p. 239~241 °C; ¹H NMR (DMSO-*d*₆, 400 MHz): δ_{H} 8.60 (d, *J* = 3.0 Hz, 1H), 7.98–7.91 (m, 1H), 7.90–7.85 (m, 1H), 7.75 (d, *J* = 2.8 Hz, 1H), 7.71–7.66 (m, 2H), 7.60–7.52 (m, 2H), 7.10 (d, *J* = 8.9 Hz, 1H), 6.81 (d, *J* = 2.3 Hz, 1H), 6.49 (d, *J* = 2.3 Hz, 1H), 4.17 (t, *J* = 6.3 Hz, 2H), 4.00 (t, *J* = 6.2 Hz, 2H), 3.89 (s, 3H), 3.84 (d, *J* = 2.4 Hz, 6H), 3.80 (s, 3H), 1.97–1.81 (m, 4H). ¹³C NMR (DMSO-*d*₆, 100 MHz): δ_{C} 172.7, 164.1, 160.8, 158.7, 158.6, 152.6, 152.4, 151.1, 148.8, 144.7, 143.3, 139.9, 129.2, 129.1, 127.5, 127.0, 123.1, 121.9, 113.7, 111.8, 111.6, 108.9, 96.4, 93.5, 71.5, 68.0, 56.6, 56.51, 56.50, 56.0, 26.6, 25.7. IR (KBr): ν 3001, 2938, 2838, 1637, 1514, 1490, 1463, 1348, 1322, 1212, 1108, 1023, 912, 872, 820, 782, 753, 709, 667, 647 cm^{-1} . HRMS (ESI, m/z): Calcd for $\text{C}_{32}\text{H}_{32}\text{NO}_8$ [M + H]⁺ 558.2128, found 558.2113.

2-(3,4-dimethoxyphenyl)-5,7-dimethoxy-3-(4-(quinolin-4-yloxy)butoxy)-4H-chromen-4-one (3m): CC (EA/ET = 11: 1). Yield 79%, M.p. 233~234 °C; ¹H NMR (DMSO-*d*₆, 400 MHz): δ_{H} 8.70 (d, *J* = 5.1 Hz, 1H), 8.10 (dd, *J* = 0.9, 8.3 Hz, 1H), 7.93 (d, *J* = 8.3 Hz, 1H), 7.77–7.66 (m, 3H), 7.53 (ddd, *J* = 1.1, 7.0, 8.2 Hz, 1H), 7.08 (d, *J* = 9.0 Hz, 1H), 6.99 (d, *J* = 5.3 Hz, 1H), 6.82 (d, *J* = 2.3 Hz, 1H), 6.49 (d, *J* = 2.3 Hz, 1H), 4.27 (t, *J* = 6.2 Hz, 2H), 4.03 (t, *J* = 6.2 Hz, 2H), 3.90 (s, 3H), 3.84 (s, 3H), 3.81 (s, 3H), 3.79 (s, 3H), 2.02–1.95 (m, 2H), 1.94–1.87 (m, 2H). ¹³C NMR (DMSO-*d*₆, 100 MHz): δ_{C} 172.7, 164.2, 161.1, 160.8, 158.7, 152.4, 152.1, 151.1, 149.2, 148.8, 139.9, 130.1, 129.1, 126.1, 123.1, 121.9, 121.3, 120.0, 111.84, 111.80, 109.0, 102.0, 96.4, 93.5, 71.6, 68.4, 56.6, 56.5, 56.1, 56.0, 26.7, 25.6. IR (KBr): ν 3060, 2996, 2954, 2838, 1629, 1514, 1463, 1382, 1311, 1267, 1212, 1109, 990, 979, 955, 863, 798, 796, 757, 666, 649 cm^{-1} . HRMS (ESI, m/z): Calcd for $\text{C}_{32}\text{H}_{32}\text{NO}_8$ [M + H]⁺ 558.2128, found 558.2109.

2-(3,4-dimethoxyphenyl)-5,7-dimethoxy-3-(4-(quinolin-6-yloxy)butoxy)-4H-chromen-4-one (3n): CC (EA/ET = 10: 1). Yield 83%, M.p. 239~241 °C; ¹H NMR (DMSO-*d*₆, 400 MHz): δ_{H} 8.72 (dd, *J* = 1.7, 4.2 Hz, 1H), 8.23 (dd, *J* = 1.0, 8.4 Hz, 1H), 7.93–7.88 (m, 1H), 7.73–7.66 (m, 2H), 7.46 (dd, *J* = 4.2, 8.3 Hz, 1H), 7.39–7.34 (m, 2H), 7.10 (d, *J* = 9.0 Hz, 1H), 6.82 (d, *J* = 2.3 Hz, 1H), 6.49 (d, *J* = 2.3 Hz, 1H), 4.13 (t, *J* = 6.1 Hz, 2H), 4.00 (t, *J* = 6.1 Hz, 2H), 3.89 (s, 3H), 3.84 (d, *J* = 2.0 Hz, 6H), 3.81 (s, 3H), 1.96–1.80 (m, 4H). ¹³C NMR (DMSO-*d*₆, 100 MHz): δ_{C} 172.7, 164.1, 160.8, 158.7, 156.9, 152.4, 151.1, 148.8, 148.3, 144.2, 139.9, 135.2, 130.8, 129.5, 123.1, 122.6, 122.1, 121.9, 111.9, 111.7, 108.9, 106.8, 96.4, 93.5, 71.5, 67.9, 56.6, 56.5, 56.1, 56.0, 26.7, 25.8. IR (KBr): ν 3083, 2947, 2873, 1629, 1575, 1515, 1464, 1428, 1404, 1379, 1360, 1267, 1212, 1144, 1106, 1075, 1021, 975, 865, 824, 797, 785, 768, 650, 617 cm^{-1} . HRMS (ESI, m/z): Calcd for $\text{C}_{32}\text{H}_{32}\text{NO}_8$ [M + H]⁺ 558.2128, found 558.2108.

2-(3,4-dimethoxyphenyl)-5,7-dimethoxy-3-(4-(quinolin-7-yloxy)butoxy)-4H-chromen-4-one (3o): CC (EA/ET = 10: 1). Yield 75%, M.p. 203~205 °C; ¹H NMR (DMSO-*d*₆, 400 MHz): δ_{H} 8.80 (dd, *J* = 1.7, 4.3 Hz, 1H), 8.26 (dd, *J* = 1.4, 8.3 Hz, 1H), 7.87 (d, *J* = 9.0 Hz, 1H), 7.72–7.66 (m, 2H), 7.39–7.33 (m, 2H), 7.22 (dd, *J* = 2.5, 8.9 Hz, 1H), 7.11 (d, *J* = 8.4 Hz, 1H), 6.82 (d, *J* = 2.3 Hz, 1H), 6.49 (d, *J* = 2.3 Hz, 1H), 4.16 (t, *J* = 6.0 Hz, 2H), 4.00 (t, *J* = 6.1 Hz, 2H), 3.89 (s, 3H), 3.84 (s, 6H), 3.81 (s, 3H), 1.94–1.83 (m, 4H). ¹³C NMR (DMSO-*d*₆, 100 MHz): δ_{C} 172.7, 164.1, 160.8, 159.9, 158.7, 152.4, 151.2, 151.1, 149.9, 148.8, 139.9, 136.1, 129.7, 123.5, 123.1, 121.9, 119.9, 119.6, 111.9, 111.8, 109.0, 108.3, 96.4, 93.5, 71.6, 67.9, 56.6, 56.5, 56.1, 56.0, 26.7, 25.8. IR (KBr): ν 3003, 2935, 2840, 1633, 1513, 1456, 1428, 1346, 1322, 1270, 1246, 1212, 1163, 1134, 1057, 1034, 1021, 979, 865, 838, 817, 767, 732, 663, 617 cm^{-1} . HRMS (ESI, m/z): Calcd for $\text{C}_{32}\text{H}_{32}\text{NO}_8$ [M + H]⁺ 558.2128, found 558.2111.

3.4. Cell Proliferative Assay

3.4.1. Cell Growth Conditions and Antiproliferative Assay for Human Cancer Cell Lines

DDP was selected as the positive control drug, and the inhibitory effect of the synthesized quercetin derivatives containing quinoline groups on HepG-2, A549, and MCF-7 cell lines was evaluated by the MTS method.

All human tumor cells were cultured in RPMI 1640 medium supplemented with 10% fetal bovine serum (FBS). The cells were detached with trypsin, seeded in a 96-well plate

(5×10^4 cells per well), and incubated at 37 °C and 5% CO₂ overnight. They were then treated with the test compounds at different concentrations and incubated for 96 h. Fresh MTT solution was added to each well and incubated at 37 °C for 4 h. The MTT-formazan formed by metabolically viable cells in each well was dissolved in 150 µL DMSO and monitored by a microplate reader at a dual-wavelength of 490 nm. The IC₅₀ value was defined as the drug concentration that inhibited the cell number to 50% after 96 h. Each test was performed three times.

3.4.2. Cell Apoptosis Experiment

Cells were seeded in a 6-well plate and cultured for 24 h. The old culture medium was then removed and different concentrations of drugs in media were added, followed by incubation for 48 or 72 h. The cells were then digested with trypsin without EDTA, collected, and centrifuged. The supernatant was decanted, and PBS was added to clean the cells twice. We then added 500 µL of binding buffer per well to the resuspended cells, followed by 5 µL of Annexin V-FITC and 5 µL PI were then gently mixed and incubated at room temperature in the dark for 5–15 min. Finally, the sample was analyzed with flow cytometry. The results were quantified with Flow Jo software (v 10.8.1).

4. Conclusions

A series of quercetin derivatives bearing quinoline scaffolds were designed and synthesized. The anti-tumor activity of HepG-2, A549, and MCF-7 was evaluated via the MTT method using DDP and quercetin as positive control drugs. The results showed that some compounds modified with quercetin had increased in vitro anti-tumor activity. Target compounds **3a** and **3e** had strong inhibitory effects on all three types of tumor cells. The experiments showed that compound **3e** induced HepG-2 cell apoptosis in a concentration-dependent manner.

Supplementary Materials: The following supporting information can be downloaded at: <https://www.mdpi.com/article/10.3390/molecules29010240/s1>, Compounds characterization—Pages 2–31; ¹H NMR, ¹³C NMR, IR spectra and HRMS spectrum of all the target compounds.

Author Contributions: W.Z., R.Y., P.Z. and C.M. performed the experiments. W.Z., Y.Z. and S.D. designed the experiments and wrote the paper. H.Z., F.N. and J.S. took part in data analysis and discussion. All authors have read and agreed to the published version of the manuscript.

Funding: This research was funded by the earmarked fund for CARS-10-Sweetpotato (CARS-10), Xuzhou Science and Technology Plan Project (KC23074) and Jiangsu Province Agricultural Science and Technology Independent Innovation Fund (CX (22)2012).

Institutional Review Board Statement: Not applicable.

Informed Consent Statement: Not applicable.

Data Availability Statement: Data is contained within the article.

Conflicts of Interest: The authors declare no conflict of interest.

References

- Guven, H.; Arici, A.; Simsek, O. Flavonoids in our foods: A short review. *J. Basic Clin. Health Sci.* **2019**, *3*, 96–106. [[CrossRef](#)]
- Williamson, G.; Kay, C.D.; Crozier, A. The Bioavailability, Transport, and Bioactivity of Dietary Flavonoids: A Review from a Historical Perspective. *Compr. Rev. Food Sci. Food Saf.* **2018**, *17*, 1054–1112. [[CrossRef](#)] [[PubMed](#)]
- Shen, N.; Wang, T.; Gan, Q.; Liu, S.; Wang, L.; Jin, B. Plant flavonoids: Classification, distribution, biosynthesis, and antioxidant activity. *Food Chem.* **2022**, *383*, 132531. [[CrossRef](#)] [[PubMed](#)]
- Ezzati, M.; Yousefi, B.; Velaei, K.; Safa, A. A review on anti-cancer properties of Quercetin in breast cancer. *Life Sci.* **2020**, *248*, 117463. [[CrossRef](#)] [[PubMed](#)]
- Tang, S.M.; Deng, X.T.; Zhou, J.; Li, Q.P.; Ge, X.X.; Miao, L. Pharmacological basis and new insights of quercetin action in respect to its anti-cancer effects. *Biomed. Pharmacother.* **2020**, *121*, 109604. [[CrossRef](#)] [[PubMed](#)]

6. Wu, L.; Li, J.; Liu, T.; Li, S.; Feng, J.; Yu, Q.; Zhang, J.; Chen, J.; Zhou, Y.; Ji, J.; et al. Quercetin shows anti-tumor effect in hepatocellular carcinoma LM3 cells by abrogating JAK2/STAT3 signaling pathway. *Cancer Med.* **2019**, *8*, 4806–4820. [CrossRef] [PubMed]
7. Li, Y.; Yao, J.; Han, C.; Yang, J.; Chaudhry, M.T.; Wang, S.; Liu, H.; Yin, Y. Quercetin, Inflammation and Immunity. *Nutrients* **2016**, *8*, 167. [CrossRef]
8. Hou, D.D.; Zhang, W.; Gao, Y.L.; Sun, Y.Z.; Wang, H.X.; Qi, R.Q.; Chen, H.D.; Gao, X.H. Anti-inflammatory effects of quercetin in a mouse model of MC903-induced atopic dermatitis. *Int. Immunopharmacol.* **2019**, *74*, 105676. [CrossRef]
9. Di Petrillo, A.; Orrù, G.; Fais, A.; Fantini, M.C. Quercetin and its derivates as antiviral potentials: A comprehensive review. *Phytother. Res.* **2022**, *36*, 266–278. [CrossRef]
10. Shohan, M.; Nashibi, R.; Mahmoudian-Sani, M.R.; Abolnezhadian, F.; Ghafourian, M.; Alavi, S.M.; Sharhani, A.; Khodadadi, A. The therapeutic efficacy of quercetin in combination with antiviral drugs in hospitalized COVID-19 patients: A randomized controlled trial. *Eur. J. Pharmacol.* **2022**, *914*, 174615. [CrossRef]
11. Zaragozá, C.; Monserrat, J.; Mantecón, C.; Villaescusa, L.; Álvarez-Mon, M.Á.; Zaragozá, F.; Álvarez-Mon, M. Binding and antiplatelet activity of quercetin, rutin, diosmetin, and diosmin flavonoids. *Biomed. Pharmacother.* **2021**, *141*, 111867. [CrossRef] [PubMed]
12. Liu, H.L.; Jiang, W.B.; Xie, M.X. Flavonoids: Recent advances as anticancer drugs. *Recent Pat. Anticancer Drug Discov.* **2010**, *52*, 152–164. [CrossRef]
13. Vue, B.; Zhang, S.; Chen, Q.H. Synergistic Effects of Dietary Natural Products as Anti-Prostate Cancer Agents. *Nat. Prod. Commun.* **2015**, *10*, 2179–2188. [CrossRef] [PubMed]
14. Vue, B.; Zhang, S.; Chen, Q.H. Flavonoids with Therapeutic Potential in Prostate Cancer. *Anticancer Agents Med. Chem.* **2016**, *16*, 1205–1229. [CrossRef] [PubMed]
15. Rajaram, P.; Jiang, Z.; Chen, G.; Rivera, A.; Phasakda, A.; Zhang, Q.; Zheng, S.; Wang, G.; Chen, Q.H. Nitrogen-containing derivatives of O-tetramethylquercetin: Synthesis and biological profiles in prostate cancer cell models. *Bioorg. Chem.* **2019**, *87*, 227–239. [CrossRef] [PubMed]
16. Yuan, J.; Wong, I.L.; Jiang, T.; Wang, S.W.; Liu, T.; Wen, B.J.; Chow, L.M.; Wan, S.B. Synthesis of methylated quercetin derivatives and their reversal activities on P-gp- and BCRP-mediated multidrug resistance tumour cells. *Eur. J. Med. Chem.* **2012**, *54*, 413–422. [CrossRef] [PubMed]
17. Zizkova, P.; Stefk, M.; Rackova, L.; Prnova, M.; Horakova, L. Novel quercetin derivatives: From redox properties to promising treatment of oxidative stress related diseases. *Chem. Biol. Interact.* **2017**, *265*, 36–46. [CrossRef] [PubMed]
18. Magar, R.T.; Sohng, J.K. A Review on Structure, Modifications and Structure-Activity Relation of Quercetin and Its Derivatives. *J. Microbiol. Biotechnol.* **2020**, *30*, 11–20. [CrossRef]
19. Aboelnaga, A.; EL-Sayed, T.H. Click synthesis of new 7-chloroquinoline derivatives by using ultrasound irradiation and evaluation of their biological activity. *Green Chem. Lett. Rev.* **2018**, *11*, 254–263. [CrossRef]
20. Amoozgar, Z. Design, synthesis, and biological evaluation of novel quinoline-based molecules with potential anticancer activity. *Chem. Biol. Drug. Des.* **2016**, *88*, 585–591.
21. Abadi, A.H.; Hegazy, G.H.; El-Zaher, A.A. Synthesis of novel 4-substituted-7-trifluoromethylquinoline derivatives with nitric oxide releasing properties and their evaluation as analgesic and antiinflammatory agents. *Bioorg. Med. Chem.* **2005**, *13*, 5759–5765. [CrossRef] [PubMed]
22. Chen, Y.L.; Zhao, Y.L.; Lu, C.M.; Tzeng, C.C.; Wang, J.P. Synthesis, cytotoxicity, and anti-inflammatory evaluation of 2-(furan-2-yl)-4-(phenoxy)quinoline derivatives. Part 4. *Bioorg. Med. Chem.* **2006**, *14*, 4373–4378. [CrossRef] [PubMed]
23. Lenoci, A.; Tomassi, S.; Conte, M.; Benedetti, R.; Rodriguez, V.; Carradori, S.; Secci, D.; Castellano, S.; Sbardella, G.; Filetici, P.; et al. Quinoline-based p300 histone acetyltransferase inhibitors with pro-apoptotic activity in human leukemia U937 cells. *Chem. Med. Chem.* **2014**, *9*, 542–548. [CrossRef] [PubMed]
24. Dorababu, A. Recent update on antibacterial and antifungal activity of quinoline scaffolds. *Arch. Pharm.* **2021**, *354*, e2000232. [CrossRef] [PubMed]
25. de la Guardia, C.; Stephens, D.E.; Dang, H.T.; Quijada, M.; Larionov, O.V.; Lleonart, R. Antiviral activity of novel quinoline derivatives against dengue virus serotype 2. *Molecules* **2018**, *23*, 672. [CrossRef] [PubMed]
26. Han, Y.; Pham, H.T.; Xu, H.; Quan, Y.; Mesplède, T. Antimalarial drugs and their metabolites are potent Zika virus inhibitors. *J. Med. Virol.* **2019**, *91*, 1182–1190. [CrossRef]
27. Kos, J.; Ku, C.F.; Kapustikova, I.; Oravec, M.; Zhang, H.-J.; Jampilek, J. 8-hydroxyquinoline-2-carboxanilides as antiviral agents against avian influenza virus. *Chem. Sel.* **2019**, *4*, 4582–4587. [CrossRef]
28. Singh, A.K.; Singh, A.; Shaikh, A.; Singh, R.; Misra, A. Chloroquine and hydroxychloroquine in the treatment of COVID-19 with or without diabetes: A systematic search and a narrative review with a special reference to India and other developing countries. *Diabetes Metab. Syndr.* **2020**, *14*, 241–246. [CrossRef]
29. Gao, J.; Tian, Z.; Yang, X. Breakthrough: Chloroquine phosphate has shown apparent efficacy in treatment of COVID-19 associated pneumonia in clinical studies. *Biosci. Trends* **2020**, *14*, 72–73. [CrossRef]
30. Al-Jabban, S.M.; Zhang, X.; Chen, G.; Mekuria, E.A.; Rakotondraibe, L.H.; Chen, Q.H. Synthesis and Anti-Proliferative Effects of Quercetin Derivatives. *Nat. Prod. Commun.* **2015**, *10*, 2113–2118. [CrossRef]

31. Liu, T.; Peng, F.; Cao, X.; Liu, F.; Wang, Q.; Liu, L.; Xue, W. Design, Synthesis, Antibacterial Activity, Antiviral Activity, and Mechanism of Myricetin Derivatives Containing a Quinazolinone Moiety. *ACS Omega* **2021**, *6*, 30826–30833. [[CrossRef](#)] [[PubMed](#)]
32. Xue, W.; Song, B.A.; Zhao, H.J.; Qi, X.B.; Huang, Y.J.; Liu, X.H. Novel myricetin derivatives: Design, synthesis and anticancer activity. *Eur. J. Med. Chem.* **2015**, *97*, 155–163. [[CrossRef](#)] [[PubMed](#)]
33. Jiang, S.; Su, S.; Chen, M.; Peng, F.; Zhou, Q.; Liu, T.; Liu, L.; Xue, W. Antibacterial Activities of Novel Dithiocarbamate-Containing 4H-Chromen-4-one Derivatives. *J. Agric. Food Chem.* **2020**, *68*, 5641–5647. [[CrossRef](#)] [[PubMed](#)]
34. Jiang, S.; Tang, X.; Chen, M.; He, J.; Su, S.; Liu, L.; He, M.; Xue, W. Design, synthesis and antibacterial activities against *Xanthomonas oryzae* pv. *oryzae*, *Xanthomonas axonopodis* pv. *Citri* and *Ralstonia solanacearum* of novel myricetin derivatives containing sulfonamide moiety. *Pest Manag. Sci.* **2020**, *76*, 853–860. [[CrossRef](#)]
35. Liu, F.; Cao, X.; Zhang, T.; Xing, L.; Sun, Z.; Zeng, W.; Xin, H.; Xue, W. Synthesis and Biological Activity of Myricetin Derivatives Containing Pyrazole Piperazine Amide. *Int. J. Mol. Sci.* **2023**, *24*, 10442. [[CrossRef](#)]

Disclaimer/Publisher's Note: The statements, opinions and data contained in all publications are solely those of the individual author(s) and contributor(s) and not of MDPI and/or the editor(s). MDPI and/or the editor(s) disclaim responsibility for any injury to people or property resulting from any ideas, methods, instructions or products referred to in the content.